

Spontaneous, collective coherence in driven, dissipative cavity arrays

J. Ruiz-Rivas,¹ E. del Valle,^{2,*} C. Gies,³ and M. J. Hartmann^{4,5}

¹*Departament d'Òptica, Universitat de València, Dr. Moliner 50, 46100 Burjassot, Spain*

²*Física Teórica de la Materia Condensada, Universidad Autónoma de Madrid, 28049 Madrid, Spain*

³*Institute for Theoretical Physics, University of Bremen, 28334 Bremen, Germany*

⁴*Institute of Photonics and Quantum Sciences, Heriot-Watt University, Edinburgh, EH14 4AS, United Kingdom*

⁵*Technische Universität München, Physik Department, James Franck Str., 85748 Garching, Germany*

(Dated: December 3, 2024)

We study an array of dissipative tunnel-coupled cavities, each interacting with an incoherently pumped two-level emitter. For cavities in the lasing regime, we find correlations between the light fields of distant cavities, despite the dissipation and the incoherent nature of the pumping mechanism. These correlations decay exponentially with distance for arrays in any dimension but become increasingly long ranged with increasing photon tunneling between adjacent cavities. The interaction-dominated and the tunneling-dominated regimes show markedly different scaling of the correlation length which always remains finite due to the finite photon trapping time. We propose a series of observables to characterize the spontaneous build-up of collective coherence in the system.

PACS numbers: 67.25.dj, 42.50.Ct, 64.60.Ht, 42.55.Ah

Arrays of optical or microwave cavities, each interacting strongly with quantum emitters and mutually coupled via the exchange of photons, have been introduced as prototype setups for the study of quantum many-body physics of light [1–3]. Even though ground or thermal equilibrium states of the corresponding quantum many-body systems are challenging to generate in experiments, much of the initial attention has focussed on this regime, see e.g. the reviews [4–7]. In any realistic experiment with cavity arrays, however, photons are dissipated due to the imperfect confinement of the light, and emitter excitations have finite lifetimes. It is thus crucial and useful to explore the driven-dissipative regime of these structures, where photon losses are continuously compensated by pumping new photons into the cavities. A special role is here taken by the stationary states where photon pumping and losses balance each other in a *dynamical equilibrium*. The driven-dissipative regime of coupled cavity arrays has thus received considerable attention in recent years, where coherent and strongly correlated phases have been discovered [8–10], but also analogies to quantum Hall physics [11] and topologically protected quantum states [12] have been discussed.

In previous investigations of coupled cavity arrays in driven-dissipative regimes, the pump mechanism that injects photons into the array has been assumed to be a coherent drive at each cavity [8–12]. Therefore any phase-coherence between light fields in distant cavities that was seen in these studies can at least in part be attributed to the fixed phase relation between their coherent input drives. Here, in contrast, we show that such a coherence between distant cavities can build up spontaneously, triggered only by physical processes within the array. In this way we address the question of whether a non-equilibrium superfluid can develop in these structures. To this end, we consider a cavity array that is only

driven by an incoherent pump which explicitly avoids any external source for a preferred phase relation between photons in different cavities.

In our model, the cavities are mutually coupled via the exchange of photons and each strongly interacts with a two-level emitter. Whereas both, emitters and cavity photons, are subject to dissipation processes, the cavities are excited via the emitters only, which are population inverted by an incoherent pump. For a single cavity our model reduces to the previously considered and realized case of a *one-emitter laser* [13–17]. Generalizations of this single cavity model have also been studied for two [18] and multiple emitters [19–21] or emitters supporting multi-exciton states [22].

We focus our analysis on the build-up of first-order coherence between the fields in distant cavities as this quantity is typically considered for investigating long range order and the emergence of superfluidity, e.g. in optical lattices [23]. In cavity arrays these correlations can be measured by recording the interference pattern of the light fields emitted from the individual cavities. We find that collective correlations indeed build up in our set-up when the cavities are in the lasing regime. These correlations decay exponentially as the distance between the considered cavities tends to infinity for any dimension of the array. As intuitively expected, the associated correlation length increases with increasing photon tunneling between the cavities. For the interaction-dominated regime this increase is logarithmic, whereas it is a power law in the tunneling-dominated regime. Nonetheless, for any non-vanishing cavity decay rate, the correlation length always remains finite.

Related questions are of high relevance in systems with engineered dissipation [24–26] or exciton-polariton condensates [7], where, using a functional renormalization group approach, correlations were found to decay ex-

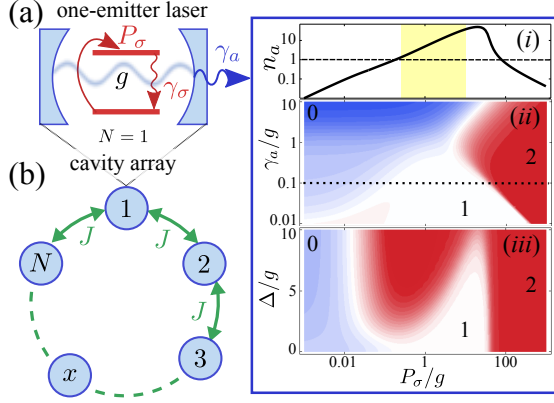


FIG. 1. (Color online) (a) The building block of the array, the one-emitter laser and its main cavity emission properties: (i) cavity population n_a as a function of P_σ for $\gamma_a = 0.1g$ and $\Delta = 0$, with the lasing region highlighted in yellow. Below, contour plots of $g^{(2)}$ as a function of P_σ and γ_a at $\Delta = 0$ (ii) and as a function of P_σ and Δ at $\gamma_a = 0.1g$ (iii). Red regions correspond to $g^{(2)} > 1$, white to $g^{(2)} = 1$ and blue to $g^{(2)} < 1$. In these figures, $\gamma_\sigma = 0.01g$ and $J = 0$. (b) Scheme of the total system in one dimension: a circular array of N coupled cavities containing a single emitter each.

ponentially in isotropic two-dimensional [27] but algebraically in three-dimensional systems [28].

Finally, we also find that the collective coherence build-up manifests strongly in the local properties for each cavity, such as intensity and spectrum of emission. In particular, lasing and its typical photoluminescence lineshape, the Mollow triplet [17, 29], can be observed far out of resonance between emitter and cavity as a result of the emergence of collective photonic modes.

Suitable experimental platforms for exploring our findings are for example superconducting circuit [6], photonic crystal [30, 31], micro-pillar [32], and waveguide coupled cavities [33].

Model— We consider an array of cavities with a Jaynes-Cummings interaction between a two level emitter and the photons in each cavity and photon tunneling between adjacent cavities. Our system, c.f. Fig. 1(a) and (b), is thus described by a Jaynes-Cummings-Hubbard Hamiltonian ($\hbar = 1$),

$$H = \sum_j H_j^{JC} + \sum_{\langle j,l \rangle} J[a_j^\dagger a_l + a_l^\dagger a_j] \quad \text{with} \quad (1)$$

$$H_j^{JC} = \omega_a a_j^\dagger a_j + \omega_\sigma \sigma_j^\dagger \sigma_j + g(a_j^\dagger \sigma_j + a_j \sigma_j^\dagger),$$

where a_j is the photon annihilation operator and $\sigma_j = |g\rangle_j \langle e|_j$ the emitter de-excitation operator in cavity j . We assume periodic boundary conditions and a homogeneous array with photon tunneling rate J so that all H_j^{JC} feature the same photon frequency ω_a , emitter transition frequency ω_σ , and light-matter coupling g . We are here interested in a driven-dissipative regime, where each emitter is excited by an incoherent pump at a rate

P_σ [34], and decays spontaneously at a rate γ_σ . The cavity photons in turn are lost at a rate γ_a from each cavity. We thus describe the dynamics of our system, including these incoherent processes, with the master equation,

$$\partial_t \rho = -i[H, \rho] + \sum_j [\gamma_a \mathcal{L}_{a_j} + \gamma_\sigma \mathcal{L}_{\sigma_j} + P_\sigma \mathcal{L}_{\sigma_j^\dagger}](\rho), \quad (2)$$

where ρ is the density matrix of the total system and $\mathcal{L}_c(\rho) = \frac{1}{2}(2c\rho c^\dagger - c^\dagger c\rho - \rho c^\dagger c)$. We are interested in the steady state of Eq. (2) and neglect pure dephasing, since it does not modify the results apart from slightly increasing the decoherence that P_σ already induces.

For our analysis it is convenient to introduce Bloch modes for the photons [35], which would decompose the empty cavity version (i.e. without emitters) of the Hamiltonian (1) into a set of uncoupled harmonic modes. For a rectangular lattice of cavities of dimension m and edge length N , these modes read $p_{\vec{k}} = N^{-m/2} \sum_{\vec{r}} e^{i\vec{k} \cdot \vec{r}} a_{\vec{r}}$, where \vec{r} is an m -dimensional lattice site index and the Hamiltonian (1) takes the form

$$H = \sum_{\vec{k}} \omega_{\vec{k}} p_{\vec{k}}^\dagger p_{\vec{k}} + \sum_{\vec{r}} \omega_\sigma \sigma_{\vec{r}}^\dagger \sigma_{\vec{r}} + \sum_{\vec{k}, \vec{r}} (G_{\vec{k}\vec{r}} p_{\vec{k}} \sigma_{\vec{r}}^\dagger + \text{h.c.}), \quad (3)$$

with $\omega_{\vec{k}} = \omega_a + 2J \sum_{\alpha=1}^m \cos k_\alpha$, $G_{\vec{k}\vec{r}} = gN^{-m/2} e^{-i\vec{k} \cdot \vec{r}}$, and $k_\alpha = \frac{2\pi}{N}[-N/2 + l_\alpha]$ for N even or $k_\alpha = \frac{2\pi}{N}[-(N+1)/2 + l_\alpha]$ for N odd ($l_\alpha = 1, \dots, N$). The Bloch modes form a band with their N frequencies $\omega_{\vec{k}}$ distributed across the interval $[\omega_a - 2mJ, \omega_a + 2mJ]$. As easily seen, all modes $p_{\vec{k}}$ decay at the same rate γ_a . Hence, we have mapped our model to a set of independent harmonic modes that all couple to the same set of emitters with complex coupling constants $G_{\vec{k}\vec{r}}$. It is useful to define for each mode, the detuning $\Delta_{\vec{k}} = \omega_\sigma - \omega_{\vec{k}}$, the total decoherence rate $\Gamma = \gamma_a + P_\sigma + \gamma_\sigma$, the effective coupling $g_{\vec{k}}^{\text{eff}} = g/\sqrt{1 + (2\Delta_{\vec{k}}/\Gamma)^2}$, and the population transfer from the emitters to the mode (*Purcell rate*) $F_{\vec{k}} = 4(g_{\vec{k}}^{\text{eff}})^2/\Gamma$. Each Bloch mode can thus be driven by coherent excitation exchange with the N emitters, where the maximum effective coupling $g_{\vec{k}}^{\text{eff}}$ and thus maximum mode population is reached at resonance, $\Delta_{\vec{k}} = 0$.

Before analyzing the entire array we briefly review the properties of a single site, the one-emitter laser, which provides a guideline for the approximations we employ later. In Fig. 1(a) we show the population, $n_a = \langle a^\dagger a \rangle$, and second-order coherence function of a single cavity, $g^{(2)} = \langle a^\dagger a^\dagger a a \rangle / \langle a^\dagger a \rangle^2$ as a function of P_σ . In the strong coupling regime ($\gamma_a, \gamma_\sigma \ll g$) where we carry out our investigations, one distinguishes several regions [17]: the linear and quantum regimes at low pump ($g^{(2)} < 1$ in blue) [19, 20, 36], the lasing regime ($g^{(2)} = 1$ in white) and the self-quenching and thermal regimes at high pump ($1 < g^{(2)} \leq 2$ in red). In this work, we are mainly interested in the lasing regime, where the emitter population is roughly half-inverted, $n_\sigma = \langle \sigma^\dagger \sigma \rangle \approx n_\sigma^L = 1/2$, and

the cavity can accumulate a large number of photons, $n_a \approx n_a^L = P_\sigma/2\gamma_a$ [37]. Due to the stochastic nature of the pump, $\langle a \rangle = 0$ remains zero [38]. Instead, for the quantized light field, photon-assisted polarizations $\langle a^\dagger \sigma \rangle$ are driven [39] and induce the build-up of coherence in the cavity field (for which $\langle a^\dagger a \sigma^\dagger \sigma \rangle \approx n_a n_\sigma$). In the thermal regime, correlations between cavity field and emitter break down. This allows us to obtain simple rate equations for the populations and polarization that provide accurate results above the quantum regime, i.e. for $P_\sigma > \gamma_a, \gamma_\sigma$ [17]. The accuracy of this approach has also been confirmed for $N > 1$ emitters coupled to a single cavity mode [40].

Rate Equations— From Eq. (2), we derive an (infinite) hierarchy of coupled equations of motion for correlators [41] starting with the most relevant correlators for our purposes, $n_\sigma = \langle \sigma_{\vec{r}}^\dagger \sigma_{\vec{r}} \rangle$ and $n_{\vec{k}} = \langle p_{\vec{k}}^\dagger p_{\vec{k}} \rangle$. We then apply the cluster expansion method up to order two [39] to truncate the equations and consider the steady state $\partial_t \rho = 0$. For the lasing and thermal regimes, this approximation can be expected to be very accurate, thanks to the weak indirect interactions between modes or emitters. Hence, assuming $\langle \sigma_{\vec{r}}^\dagger \sigma_{\vec{s}} \rangle \approx n_\sigma \delta_{\vec{r}, \vec{s}}$ and $\langle p_{\vec{k}}^\dagger p_{\vec{q}} \sigma_{\vec{r}}^\dagger \sigma_{\vec{s}} \rangle \approx n_{\vec{k}} n_\sigma \delta_{\vec{k}, \vec{q}}$ (indexes \vec{r} and \vec{s} label emitters and \vec{k} and \vec{q} label Bloch modes), the populations follow the rate equations,

$$0 = -\gamma_a n_{\vec{k}} + F_{\vec{k}} n_{\vec{k}} (2n_\sigma - 1) + F_{\vec{k}} n_\sigma, \quad (4a)$$

$$0 = P_\sigma - (P_\sigma + \gamma_\sigma + F) n_\sigma - (2n_\sigma - 1) \tilde{F}, \quad (4b)$$

with $F = N^{-m} \sum_{\vec{k}} F_{\vec{k}}$ and $\tilde{F} = N^{-m} \sum_{\vec{k}} F_{\vec{k}} n_{\vec{k}}$, which are easily solved numerically. The polarizations are then given by $\langle p_{\vec{k}}^\dagger \sigma_{\vec{r}} \rangle = i G_{\vec{k}\vec{r}} (n_\sigma - n_{\vec{k}} + 2n_{\vec{k}} n_\sigma) / (\Gamma/2 + i\Delta_{\vec{k}})$ and the local cavity populations by $n_a = N^{-m} \sum_{\vec{k}} n_{\vec{k}}$. Eq. (4a) can also be formally solved for $n_{\vec{k}}$ to find

$$n_{\vec{k}} = \frac{\kappa_\sigma \Gamma}{4} \frac{n_\sigma}{(\delta/2)^2 + \Delta_{\vec{k}}^2} \quad (5)$$

with $\delta^2 = \kappa_\sigma \Gamma [\Gamma/\kappa_\sigma - (2n_\sigma - 1)]$ and $\kappa_\sigma = 4g^2/\gamma_a$, the Purcell enhanced decay of an emitter through its local cavity mode [17]. The distribution of Bloch mode populations is thus a Lorentzian in $\Delta_{\vec{k}}$ with full width at half maximum (FWHM) δ .

The central quantity of interest in our investigation are the normalized correlations between cavity fields in distant cavities,

$$\mathcal{C}(\vec{r}) = \frac{\langle a_0^\dagger a_{\vec{0}+\vec{r}} \rangle}{\langle a_0^\dagger a_{\vec{0}} \rangle} \approx \frac{1}{n_a N^m} \sum_{\vec{k}} e^{-i\vec{k} \cdot \vec{r}} n_{\vec{k}}, \quad (6)$$

where we have used that, at the present level of approximation, the Bloch modes are uncorrelated, $\langle p_{\vec{k}}^\dagger p_{\vec{q}} \rangle \approx \delta_{\vec{k}, \vec{q}} n_{\vec{k}}$ (see Eq. (6b) in the Supplemental Material, Sec. I), implying that $\mathcal{C}(\vec{r})$ is the Fourier transform of the Bloch mode populations $n_{\vec{k}}$.

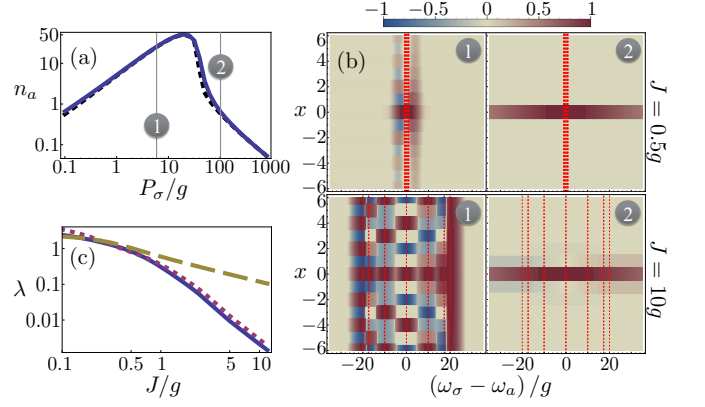


FIG. 2. (a) Cavity population n_a for $\omega_\sigma = \omega_a$ as a function of pump P_σ for $J = 0.5g$ (solid blue) and $J = 10g$ (dashed black). (b) First order correlations $\mathcal{C}(x)$ as a function of distance x and emitter frequency ω_σ for $N = 12$, $\gamma_a = 0.1g$, $\gamma_\sigma = 0.01g$ and the pump rates marked with (1) and (2) in plot (a). Bloch mode resonances are plotted as vertical dashed red lines. (c) Inverse correlations lengths, λ , as obtained from fits (see main text) for $N = 108$, $P_\sigma = 5g$, and $\Delta = 0$ (solid), $\Delta = J$ (dotted) or $\Delta = 2J$ (dashed).

Asymptotics of Correlations— Inserting Eq. (5) into Eq. (6), we find as a central result that the correlations $\mathcal{C}(\vec{r})$ decay exponentially in distance $r = |\vec{r}|$ provided $\delta \neq 0$. That is, they decay faster than r^{-n} as $r \rightarrow \infty$ for any positive integer n and lattice dimension m . The proof of this statement is provided in the Supplemental Material, Sec. II, and proceeds by showing, via multiple applications of the divergence theorem, that $\int d^m r r^{2n} |\mathcal{C}(\vec{r})|^2$ is finite for any positive integer n . The only possibility for the system to become critical, in the sense that the correlation length of $|\mathcal{C}(\vec{r})|$ diverges, would be that δ vanishes, i.e. that $\Gamma/\kappa_\sigma = (2n_\sigma - 1)$. It is however easily seen that the last term in Eq. (4b) diverges for $N \rightarrow \infty$ unless $(2n_\sigma - 1) \rightarrow 0$, which would imply $\gamma_a = 0$ for $\delta = 0$. We thus conclude that any non-vanishing photon decay rate keeps the correlation length finite and thus prevents criticality.

Correlations in one dimension— We now turn to study correlations for the case of a one-dimensional chain, $\mathcal{C}(x)$ with $-N/2 \leq x \leq N/2$, see Eq. (6), which are real since $n_k = n_{-k}$ for all $k \neq 0, \pi$. We here choose N to be a multiple of 4, so that $\omega_{k=\pm\pi/2} = \omega_a$ and Bloch modes are distributed symmetrically around the cavity frequency with their populations independent of the sign of Δ . We first focus on $N = 12$ and the two tunneling rates, $J = 0.5g$ and $J = 10g$, for which we show the total cavity population as a function of the pump in Fig. 2(a). Both cases undergo a very similar and characteristic transition into and out of lasing (compare to Fig. 1(a)-(i)). We thus choose two pumping rates representative for the lasing (1) and thermal (2) regimes and plot in Fig. 2(b) the correlations $\mathcal{C}(x)$ as a function of

detuning $\Delta = \omega_\sigma - \omega_a$ and the separation x between the cavities. For $|\Delta| < 2J$, they oscillate as $\cos(kx)$, where \bar{k} and $-\bar{k}$ are the (degenerate) modes closest to resonance with the emitters, i.e. $|\Delta| \approx 2J \cos \bar{k}$. As Fig. 2(b) shows the correlation length is longer in the lasing regime (1) and increases for larger tunneling rates J . In each case the correlation length becomes maximal for $|\Delta| = 2J$, i.e. when the emitters are in resonance with the edges of the Bloch band. For $J = 10g$ the correlation length becomes larger than the finite size array of $N = 12$ considered here since the frequency separation between Bloch modes is so large that the emitters only populate one mode efficiently. Note that within our approximations, any decay of correlations is entirely due to destructive interference between different Bloch-mode contributions.

Let us now focus on the regime $|\Delta| \leq 2J$, where the emitters are on resonance with the Bloch band and photonic modes are appreciably populated. For a long chain, $N \gg 1$, and large tunneling rates, $J \gg g$, analytical estimates can be found for the correlations $\mathcal{C}(x)$ (see the Supplemental Material, Sec. II). In agreement with Fig. 2, these show exponential decay modulated by an oscillation. To analyze the correlations further, we fit a function $f(x) = [c_1 \cos(\nu x) + c_2 \sin(\nu x)] \exp(-\lambda x)$ to $\mathcal{C}(x)$ in the entire range of tunneling rates J and extract the inverse correlation length λ from the fit (see the Supplemental Material, Sec. II, for examples of the fits). Fig. 2(c) shows λ for three cases: $\Delta = 0$ (solid), $\Delta = J$ (dotted) and $\Delta = 2J$ (dashed) for a chain of $N = 108$ cavities, which has Bloch modes in resonance with the emitters for all considered values of Δ so that finite-size effects are avoided. As second main result of our work we observe a clear transition from the regime with $J < g$, where $\lambda \propto -\ln J$, to the regime $J > g$, where $\lambda \propto J^{-1}$ for $J \gg |\Delta|$ and $\lambda \propto J^{-1/2}$ for $2J = |\Delta|$ (see the Supplemental Material, Sec. II, for the derivations). Yet, as the fit quality decreases for $J \rightarrow 0$, the scaling in this regime needs to be interpreted with some caution.

Local properties in one-dimensional chains— Finally, we present some experimentally observable local signatures of the collective lasing regime in the array. In particular, the emission properties show very distinctive features as a function of detuning. In Fig. 3(a)–(i) we plot the populations of the cavities n_a (solid blue lines) and emitters n_σ (solid purple lines), computed from the rate equations. Each underlying Bloch mode n_k (thin lines) enters its own lasing regime at $\omega_\sigma = \omega_k$ (vertical dashed red lines). This results in the enhancement of n_a to a fixed value, given approximately by the resonant one-emitter case n_a^L (dashed blue line), while the emitter population decreases to $n_\sigma^L \approx 1/2$ from its saturation value of 1 and $g^{(2)} \approx 1$ although our rate equations do not provide this information. Note that these traits are independent of g , N and J once the system is strongly enough coupled to reach the lasing regime [42]. With these conditions we compare various arrays, i.e. $N = 4$,

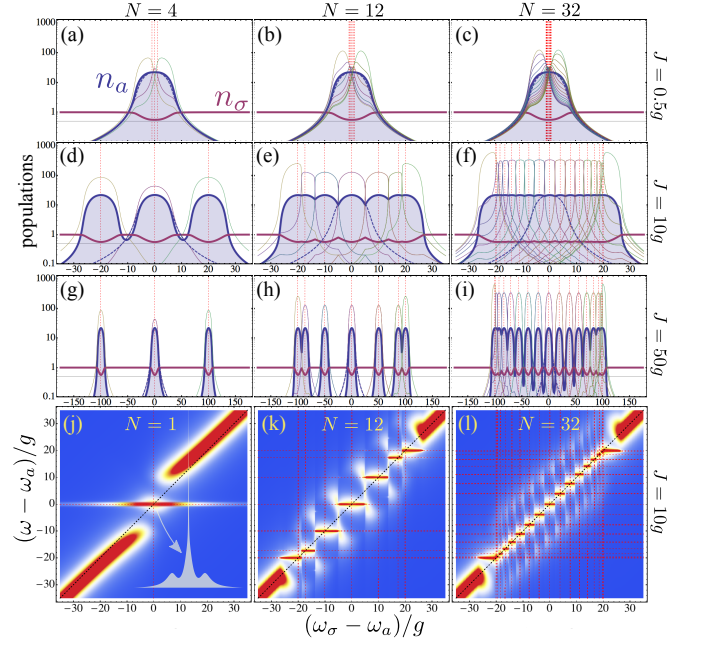


FIG. 3. (a)–(i) Populations of the different modes involved, when sweeping the emitter frequency ω_σ through the system resonances (marked with vertical red dashed lines): n_a in solid and filled blue, n_σ in solid pink, the Bloch modes n_k with thin lines and n_a for the case $N = 1$ in dashed blue as a reference. (j) Emitter spectrum of emission for the one-emitter laser, $N = 1$, for varying ω_σ , showing a Mollow triplet around resonance. In inset, the lineshape at resonance. In (k) and (l), the spectra for cases (e) and (f), respectively. We use a temperature color code which goes from blue (0) to red (maximum values). Parameters are $N = 4, 12, 32$ and $J = 0.5g, 10g, 50g$, varying as indicated. Also: $P_\sigma = 5g$ (lasing regime), $\gamma_a = 0.1g$, $\gamma_\sigma = 0.01g$ (strong coupling regime), $\Gamma_d = 0.3g$.

12, 32 and $J/g = 0.5, 10, 50$, and the one-emitter laser (showing n_a only for that case), see Fig. 3.

Interactions as small as $J \lesssim 0.5g$ (Fig. 3 upper row) are not enough to make a qualitative difference to the $N = 1$ case in the local populations (the rate equations provide for this case an analytical solution, c.f. Eq. (10) in the Supplemental Material, Sec. I). The width in detuning of the apparent single broad resonance is given approximately by $2\Delta_{\max} = \sqrt{P_\sigma(\kappa_\sigma - P_\sigma)}$ [43]. Increasing interactions, $J > g$ (middle rows), splits the Bloch modes apart so that they can be selectively and precisely addressed by changing detuning. The excitation is distributed equally among the modes that are being driven so, at resonance, we have $n_{k=0,\pi} = Nn_a^L$ at the edges of the Bloch band and $n_{\pm k} = Nn_a^L/2$ for the other modes. In Fig. 3(d)–(i) one can appreciate the two different values for the Bloch populations, at the extreme or central resonances. This results in a series of peaks for n_a of equal height n_a^L and width $2\Delta_{\max}$. When the width is smaller than the average separation between Bloch modes, which is approximately given by $4J/N$ (or

$4J/(N-1)$ for odd N), a plateau forms in the populations that extends for detunings $|\Delta| \leq 2J$, c.f. Fig. 3(f). At this point, increasing the number of cavities N does not affect the results qualitatively.

Another revealing observable in the local system is the emitter photoluminescence spectrum $S(\Gamma_d, \omega)$ where Γ_d is the detector linewidth. In the lasing regime, we observe a modified version of resonance fluorescence [44], arising from the interplay between the incoherent pump P_σ and the coherent excitation generated during the fast exchange of excitations with the Bloch modes, that we approximately consider a multimode coherent drive $\Omega(t) = \sum_k g \sqrt{n_k/N} e^{-i\omega_k t}$ (see the Supplemental Material, Sec. III). We show the case $N = 1$ [17, 29, 45] as a reference in Fig. 3(j), varying the detuning between cavity and emitter with the celebrated Mollow triplet as it appears at resonance in the inset. In Fig. 3(k) and (l) we increase the number of cavities to $N = 12$ and $N = 32$, respectively, undergoing large interactions $J = 10g$. We require $J > g$ to have a qualitative difference from $N = 1$, in the same way as for the populations. Then, we can distinguish the formation of a Mollow triplet wherever the emitter frequency crosses a Bloch mode, as this one is the main driving field for the emitter. The Rayleigh peak, pinned at the laser frequency for a single mode excitation [44], jumps from Bloch mode to Bloch mode, depending on which one dominates the driving, in direct correspondence with the population plateaus of Fig. 3(e) and (f). The sidebands are positioned approximately at $\omega_k \pm 2\sqrt{2}g\sqrt{n_a^L}$, around resonance with a degenerate Bloch mode ω_k , and at $\omega_k \pm 2g\sqrt{n_a^L}$, around resonance with the edge modes. Therefore, in the case of high N and closely packed Bloch modes, Figs. 3(f) and (l), two Mollow continuous sidebands appear at $\omega_\sigma \pm 2\sqrt{2}g\sqrt{n_a^L}$, extending over $|\Delta| \leq 2J$. This is a very distinct feature of the array being in the collective lasing state.

Acknowledgements— JR-R acknowledges the hospitality of Technical University Munich, where part of this work was done. EdV acknowledges support from the Alexander von Humboldt-Foundation and the Spanish MINECO under contract MAT2011-22997 and MJH from the Emmy Noether grant HA 5593/1-1 and the CRC 631 (both DFG).

* elena.delvalle.reboul@gmail.com

- [1] M. J. Hartmann, F. G. S. L. Brandão, and M. B. Plenio, *Nat. Phys.* **2**, 849 (2006).
- [2] A. D. Greentree, C. Tahan, J. H. Cole, and L. C. L. Hollenberg, *Nat. Phys.* **2**, 856 (2006).
- [3] D. G. Angelakis, M. F. Santos, and S. Bose, *Phys. Rev. A* **76**, 031805 (2007).
- [4] M. Hartmann, F. Brandão, and M. Plenio, *Laser & Photonics Reviews* **2**, 527 (2008).
- [5] A. Tomadin and R. Fazio, *J. Opt. Soc. Am. B* **27**, A130 (2010).
- [6] A. A. Houck, H. E. Tureci, and J. Koch, *Nat. Phys.* **8**, 292 (2012).
- [7] I. Carusotto and C. Ciuti, *Rev. Mod. Phys.* **85**, 299 (2013).
- [8] I. Carusotto, D. Gerace, H. E. Tureci, S. De Liberato, C. Ciuti, and A. İmamoğlu, *Phys. Rev. Lett.* **103**, 033601 (2009).
- [9] M. J. Hartmann, *Phys. Rev. Lett.* **104**, 113601 (2010).
- [10] F. Nissen, S. Schmidt, M. Biondi, G. Blatter, H. E. Türeci, and J. Keeling, *Phys. Rev. Lett.* **108**, 233603 (2012).
- [11] R. O. Umucalılar and I. Carusotto, *Phys. Rev. Lett.* **108**, 206809 (2012).
- [12] C.-E. Bardyn and A. İmamoğlu, *Phys. Rev. Lett.* **109**, 253606 (2012).
- [13] Y. Mu and C. M. Savage, *Phys. Rev. A* **46**, 5944 (1992).
- [14] J. McKeever, A. Boca, A. D. Boozer, J. R. Buck, and H. J. Kimble, *Nature* **425**, 268 (2003).
- [15] O. Astafiev, K. Inomata, A. O. Niskanen, T. Yamamoto, Y. A. Pashkin, Y. Nakamura, and J. S. Tsai, *Nature* **449**, 588 (2007).
- [16] M. Nomura, N. Kumagai, S. Iwamoto, Y. Ota, and Y. Arakawa, *Nat. Phys.* **6**, 279 (2010).
- [17] E. del Valle and F. P. Laussy, *Phys. Rev. A* **84**, 043816 (2011).
- [18] G. Yeoman and G. M. Meyer, *Phys. Rev. A* **58**, 2518 (1998).
- [19] F. Laussy, A. Laucht, E. del Valle, J. J. Finley, and J. M. Villas-Bôas, *Phys. Rev. B* **84**, 195313 (2011).
- [20] A. Auffèves, D. Gerace, S. Portolan, A. Drezet, and M. F. Santos, *New J. Phys.* **13**, 093020 (2011).
- [21] A. N. Poddubny, M. M. Glazov, and N. S. Averkiev, *Phys. Rev. B* **82**, 205330 (2010).
- [22] C. Gies, M. Florian, P. Gartner, and F. Jahnke, *Opt. Express* **19**, 14370 (2011).
- [23] I. Bloch, J. Dalibard, and W. Zwerger, *Rev. Mod. Phys.* **80**, 885 (2008).
- [24] S. Diehl, A. Micheli, A. Kantian, B. Kraus, H. P. Bucheler, and P. Zoller, *Nat. Phys.* **4**, 878 (2008).
- [25] D. Marcos, A. Tomadin, S. Diehl, and P. Rabl, *New J. Phys.* **14**, 055005 (2012).
- [26] P. Schindler, M. Müller, D. Nigg, J. T. Barreiro, E. A. Martinez, M. Hennrich, T. Monz, S. Diehl, P. Zoller, and R. Blatt, *Nat. Phys.* **9**, 361 (2013).
- [27] E. Altman, L. M. Sieberer, L. Chen, S. Diehl, and J. Toner, (2013), arxiv:1311.0876.
- [28] L. M. Sieberer, S. D. Huber, E. Altman, and S. Diehl, *Phys. Rev. Lett.* **110**, 195301 (2013).
- [29] E. del Valle and F. P. Laussy, *Phys. Rev. Lett.* **105**, 233601 (2010).
- [30] A. Majumdar, A. Rundquist, M. Bajcsy, V. D. Dasika, S. R. Bank, and J. Vuckovic, *Phys. Rev. B* **86**, 195312 (2012).
- [31] A. Rundquist, A. Majumdar, M. Bajcsy, V. D. Dasika, S. Bank, and J. Vuckovic, in *CLEO: 2013* (Optical Society of America, 2013) p. CM4F.7.
- [32] M. Abbarchi, A. Amo, V. G. Sala, D. D. Solnyshkov, H. Flayac, L. Ferrier, I. Sagnes, E. Galopin, A. Lemaître, G. Malpuech, and J. Bloch, *Nat. Phys.* **9**, 275 (2013).
- [33] G. Lepert, M. Trupke, M. J. Hartmann, M. B. Plenio, and E. A. Hinds, *New J. Phys.* **13**, 113002 (2011).

- [34] E. del Valle, F. P. Laussy, and C. Tejedor, Phys. Rev. B **79**, 235326 (2009).
- [35] M. J. Hartmann, Phys. Rev. Lett. **104**, 113601 (2010).
- [36] N. Averkiev, M. Glazov, and A. Poddubny, Sov. Phys. JETP **135**, 959 (2009).
- [37] This is only below the maximum cavity population, reached at $P_\sigma \approx \kappa_\sigma/2$ [17]. We use $\gamma_a = 0.1g$, $\gamma_\sigma = 0.01g$ and $P_\sigma = 5g$ in this manuscript as a paradigmatic example of the lasing regime for any N .
- [38] K. Mølmer, Phys. Rev. A **55**, 3195 (1997).
- [39] C. Gies, J. Wiersig, M. Lorke, and F. Jahnke, Phys. Rev. A **75**, 013803 (2007).
- [40] A. Moelbjerg, P. Kaer, M. Lorke, B. Tromborg, and J. Mørk, IEEE Journal of Quantum Electronics **49**, 945 (2013).
- [41] See the Supplemental Material for a derivation of the equations of motion of the system in Sec. I.
- [42] F. Laussy, E. del Valle, and J. Finley, Proc. SPIE **8255**, 82551G (2012).
- [43] This estimation is obtained by setting to zero the approximated cavity population in the detuned one-emitter laser [17], $n_a \approx n_a^L [1 - \frac{P_\sigma}{\kappa_\sigma} (1 + (\frac{2\Delta}{P_\sigma})^2)] = 0$, and multiplying the resulting detuning by 2.
- [44] B. R. Mollow, Phys. Rev. **188**, 1969 (1969).
- [45] E. del Valle and F. P. Laussy, Wolfram Demonstrations Project (2013).
- [46] E. del Valle, *Microcavity Quantum Electrodynamics* (VDM Verlag, 2010).
- [47] A. Gonzalez-Tudela, E. del Valle, E. Cancellieri, C. Tejedor, D. Sanvitto, and F. P. Laussy, Opt. Express **18**, 7002 (2010).
- [48] J. Eberly and K. Wódkiewicz, J. Opt. Soc. Am. **67**, 1252 (1977).
- [49] J. H. Eberly, C. V. Kunasz, and K. Wódkiewicz, J. phys. B.: At. Mol. Phys. **13**, 217 (1980).
- [50] E. del Valle, A. Gonzalez-Tudela, F. P. Laussy, C. Tejedor, and M. J. Hartmann, Phys. Rev. Lett. **109**, 183601 (2012).

Supplemental Material

I. Equations of motion for the correlators

In this section, we derive the system equations of motion in the case of a one-dimensional array. They can be trivially extended to higher dimensions.

The most general operator in the system reads $\langle O \rangle = \langle \Pi_k p_k^{\dagger m_k} p_k^{n_k} \Pi_j \sigma_1^{\dagger \mu_j} \sigma_1^{\nu_j} \rangle$. From the master equation (2) in the main text, we obtain the equations of motion for the set of relevant operators by means of the general relation $\partial_t \langle O \rangle = \text{Tr}(O \partial_t \rho)$ as

$$\partial_t \langle \Pi_k p_k^{\dagger m_k} p_k^{n_k} \Pi_j \sigma_1^{\dagger \mu_j} \sigma_1^{\nu_j} \rangle = \sum_{\bar{m}_1, \bar{n}_1, \dots, \bar{\mu}_1, \bar{\nu}_1, \dots} R_{\substack{m_1, n_1, \dots, \mu_1, \nu_1, \dots \\ \bar{m}_1, \bar{n}_1, \dots, \bar{\mu}_1, \bar{\nu}_1, \dots}} \langle \Pi_k p_k^{\dagger \bar{m}_k} p_k^{\bar{n}_k} \Pi_j \sigma_1^{\dagger \bar{\mu}_j} \sigma_1^{\bar{\nu}_j} \rangle. \quad (1)$$

The diagonal elements in R , involving all modes and emitters, are given by [46]:

$$\begin{aligned} R_{\substack{m_1, n_1, \dots, \mu_1, \nu_1, \dots \\ m_1, n_1, \dots, \mu_1, \nu_1, \dots}} &= \\ &\sum_k [i\omega_k(m_k - n_k) - \frac{\gamma_a}{2}(m_k + n_k)] \\ &+ \sum_j [i\omega_\sigma(\mu_j - \nu_j) - \frac{\gamma_\sigma + P_\sigma}{2}(\mu_j + \nu_j) - \frac{\gamma_\phi}{2}(\mu_j - \nu_j)^2]. \end{aligned} \quad (2)$$

We have included in these elements the effect of pure dephasing at a rate γ_ϕ , added to the master equations through the Lindblad term $\gamma_\phi \mathcal{L}_{\sigma_j^\dagger \sigma_j}(\rho)$. This only results in the increase of the total decoherence rate into $\Gamma = \gamma_a + P_\sigma + \gamma_\sigma + \gamma_\phi$ [47]. Next, the incoherent pumping of emitter j affects only elements concerning such emitter so that for all j :

$$R_{\substack{\dots, \mu_j, \nu_j, \dots \\ \dots, \mu_j, \nu_j, \dots}} = P_\sigma \mu_j \nu_j. \quad (3)$$

Finally, the coupling between mode k and emitter j , provides the elements:

$$R_{\substack{m_k, n_k, \mu_j, \nu_j \\ m_k - 1, n_k, 1 - \mu_j, \nu_j}} = iG_{kj} m_k (1 - \mu_j), \quad (4a)$$

$$R_{\substack{m_k, n_k, \mu_j, \nu_j \\ m_k, n_k - 1, \mu_j, 1 - \nu_j}} = -iG_{kj}^* n_k (1 - \nu_j), \quad (4b)$$

$$R_{\substack{m_k, n_k, \mu_j, \nu_j \\ m_k + 1, n_k, 1 - \mu_j, \nu_j}} = iG_{kj}^* \mu_j, \quad (4c)$$

$$R_{\substack{m_k, n_k, \mu_j, \nu_j \\ m_k, n_k + 1, \mu_j, 1 - \nu_j}} = -iG_{kj} \nu_j \quad (4d)$$

$$R_{\substack{m_k, n_k, \mu_j, \nu_j \\ m_k + 1, n_k, \mu_j, 1 - \nu_j}} = -2iG_{kj}^* \mu_j (1 - \nu_j), \quad (4e)$$

$$R_{\substack{m_k, n_k, \mu_j, \nu_j \\ m_k, n_k + 1, 1 - \mu_j, \nu_j}} = 2iG_{kj} \nu_j (1 - \mu_j), \quad (4f)$$

and zero everywhere else.

With these general rules, we can write the equations for the main correlators of interest, starting with the populations of the modes, $n_k = \langle p_k^\dagger p_k \rangle$ and emitters

$$n_j = \langle \sigma_j^\dagger \sigma_j \rangle:$$

$$\partial_t n_j = -(P_\sigma + \gamma_\sigma) n_j + P_\sigma - 2 \sum_k \Im[G_{kj}^* \langle p_k^\dagger \sigma_j \rangle], \quad (5a)$$

$$\partial_t n_k = -\gamma_a n_k + 2 \sum_j \Im[G_{kj}^* \langle p_k^\dagger \sigma_j \rangle], \quad (5b)$$

$$\begin{aligned} \partial_t \langle p_k^\dagger \sigma_j \rangle &= -[\frac{\Gamma}{2} + i(\omega_\sigma - \omega_k)] \langle p_k^\dagger \sigma_j \rangle \\ &+ iG_{kj} [n_j - n_k + 2 \langle p_k^\dagger p_k \sigma_j^\dagger \sigma_j \rangle] \\ &+ \sum_{l \neq j} iG_{kl} \langle \sigma_l^\dagger \sigma_j \rangle + \sum_{q \neq k} (-iG_{ql}) \langle p_k^\dagger p_q \rangle \\ &+ \sum_{q \neq k} 2iG_{qj} \langle p_k^\dagger p_q \sigma_j^\dagger \sigma_j \rangle. \end{aligned} \quad (5c)$$

The equations for the correlators that represent the indirect coupling between different emitters or Bloch modes are:

$$\begin{aligned} \partial_t \langle \sigma_l^\dagger \sigma_j \rangle &= -(P_\sigma + \gamma_\sigma) \langle \sigma_l^\dagger \sigma_j \rangle \\ &+ \sum_k i[G_{kl}^* \langle p_k^\dagger \sigma_j \rangle - G_{kj} \langle p_k \sigma_l^\dagger \rangle] \\ &+ \sum_k 2i[G_{kj} \langle p_k \sigma_l^\dagger \sigma_j^\dagger \sigma_j \rangle - G_{kl}^* \langle p_k^\dagger \sigma_l^\dagger \sigma_l \sigma_j \rangle], \end{aligned} \quad (6a)$$

$$\begin{aligned} \partial_t \langle p_k^\dagger p_q \rangle &= -[\gamma_a - i(\omega_k - \omega_q)] \langle p_k^\dagger p_q \rangle \\ &+ \sum_j i[G_{kj} \langle p_q \sigma_j^\dagger \rangle - G_{qj}^* \langle p_k^\dagger \sigma_j \rangle]. \end{aligned} \quad (6b)$$

Finally, the intensity-intensity correlations are given by:

$$\begin{aligned} \partial_t \langle p_k^\dagger p_k \sigma_l^\dagger \sigma_l \rangle &= -(\gamma_a + P_\sigma + \gamma_\sigma) \langle p_k^\dagger p_k \sigma_l^\dagger \sigma_l \rangle + P_\sigma n_k \\ &+ i(G_{kl}^* \langle p_k^\dagger p_k p_k \sigma_l \rangle - G_{kl} \langle p_k^\dagger p_k p_k \sigma_l^\dagger \rangle) \\ &+ i \sum_{q \neq k} (G_{ql}^* \langle p_q^\dagger p_q p_k \sigma_l \rangle - G_{ql} \langle p_q^\dagger p_q p_k \sigma_l^\dagger \rangle) \\ &+ i \sum_{j \neq l} (G_{kj} \langle p_k \sigma_l^\dagger \sigma_l \sigma_j^\dagger \rangle - G_{kj}^* \langle p_k^\dagger \sigma_j \sigma_l^\dagger \sigma_l \rangle). \end{aligned} \quad (7)$$

From the Bloch mode correlators we reconstruct the correlators between the cavities, such as:

$$\langle a_j^\dagger a_{j+x} \rangle = \frac{1}{N} \sum_k e^{-ixk} [n_k + \sum_{q \neq k} e^{-i(k-q)j} \langle p_k^\dagger p_q \rangle]. \quad (8)$$

Analytical solutions of the rate equations for $N = 1$

In the case $N = 1$, we have only a single emitter and photonic mode so $F_k \rightarrow F$ and the rate equations reduce to:

$$\begin{aligned} \partial_t n_\sigma &= -(P_\sigma + \gamma_\sigma + F) n_\sigma + P_\sigma - (2n_\sigma - 1) F n_a, \\ \partial_t n_a &= -\gamma_a n_a + F n_a (2n_\sigma - 1) + F n_\sigma. \end{aligned}$$

The solution of these equations in the steady state reads:

$$n_a = \frac{F(P_\sigma - \gamma_\sigma - \gamma_a) - \gamma_a(P_\sigma + \gamma_\sigma) + \sqrt{[F(3P_\sigma + \gamma_\sigma + \gamma_a) + \gamma_a(P_\sigma + \gamma_\sigma)]^2 - 8FP_\sigma(P_\sigma + \gamma_\sigma)(F + \gamma_a)}}{4F\gamma_a}, \quad (10)$$

and $n_\sigma = (P_\sigma - \gamma_a n_a)/(P_\sigma + \gamma_\sigma)$ (which is an exact relation for $N = 1$).

II. Theorem on exponential decay of correlations

Here we consider a rectangular m -dimensional lattice of cavities in the thermodynamic limit, i.e. where infinitely many cavities are arranged in each lattice direction. We thus have an infinite number of momentum modes and approximate each $\sum_{\vec{k}}$ by an integral. We will show that the field correlations,

$$\mathcal{C}(\vec{r}) = \frac{\langle a_0^\dagger a_{\vec{0}+\vec{r}} \rangle}{\langle a_0^\dagger a_0 \rangle} = \frac{1}{n_a (2\pi)^m} \int_{V_k} d^m k e^{-i\vec{k} \cdot \vec{r}} n(\vec{k}), \quad (11)$$

always decay exponentially in the limit of large separation $r = |\vec{r}| \rightarrow \infty$. Here, V_k is the volume of a cube that extends from $-\pi$ to π in each direction, i.e. the volume of $[-\pi, \pi]^m$. To this end we consider the following quantities,

$$\mathcal{C}_\nu(\vec{r}) = \frac{1}{n_a (2\pi)^m} \int_{\mathbb{R}^m} d^m k e^{-i\vec{k} \cdot \vec{r}} n_\nu(\vec{k}), \quad (12)$$

where the k -integral now extends over the entire space of real numbers in each direction. The distributions $n_\nu(\vec{k})$

are defined as

$$n_\nu(\vec{k}) = \left[\prod_{\alpha=1}^m s(\nu, k_\alpha) \right] \tilde{n}(\vec{k}). \quad (13)$$

Here, $\tilde{n}(\vec{k}) = n(\vec{k})$ for $\vec{k} \in [-\pi, \pi]^m$ and any smooth multiple differentiable continuation of $n(\vec{k})$ otherwise, whereas $s(\nu, k_\alpha) = 1/[1 + e^{-2\nu(\pi+k_\alpha)}][1 + e^{-2\nu(\pi-k_\alpha)}]$ for $\alpha = 1, \dots, m$. With increasing integer ν , the $s(\nu, k_\alpha)$ converge to $\Theta(\pi + k_\alpha)\Theta(\pi - k_\alpha)$, where Θ denotes the Heaviside step-function. The distributions $n_\nu(\vec{k})$ thus become increasingly better approximations to $n(\vec{k})$ as ν increases. Nonetheless they are smooth and multiple differentiable for any ν , a property that we will make use of in the sequel. More precisely, for any \vec{r} and any $\varepsilon > 0$, there is an integer ν such that,

$$|\mathcal{C}(\vec{r}) - \mathcal{C}_\nu(\vec{r})| \leq \frac{1}{n_a (2\pi)^m} \int_{\mathbb{R}^m} d^m k |n(\vec{k}) - n_\nu(\vec{k})| < \varepsilon. \quad (14)$$

Hence if all $\mathcal{C}_\nu(\vec{r})$ decay exponentially as $r = |\vec{r}| \rightarrow \infty$ then also $\mathcal{C}(\vec{r})$ decays exponentially. It thus suffices to show that the $\mathcal{C}_\nu(\vec{r})$ decay faster than r^{-n} for any positive integer n as $r \rightarrow \infty$. We show this by proving that

$$\mathcal{X}_\nu^n = \int_{\mathbb{R}^m} d^m r r^{2n} |\mathcal{C}_\nu(\vec{r})|^2 \quad (15)$$

is finite for any n and any ν . Denoting $\vec{\partial}_k = (\partial/\partial k_1, \dots, \partial/\partial k_m)^T$ and applying the divergence theorem $2n$ times, we find,

$$\begin{aligned} \mathcal{X}_\nu^n &= \frac{1}{n_a^2 (2\pi)^{2m}} \int d^m r \int d^m q \int d^m k n_\nu(\vec{q}) n_\nu(\vec{k}) (-\vec{\partial}_k \cdot \vec{\partial}_k)^n e^{-i(\vec{k}-\vec{q}) \cdot \vec{r}} \\ &= \frac{1}{n_a^2 (2\pi)^{2m}} \int d^m r \int d^m q n_\nu(\vec{q}) \int d^m k [\vec{\partial}_k n_\nu(\vec{k})] \cdot \vec{\partial}_k (-\vec{\partial}_k \cdot \vec{\partial}_k)^{n-1} e^{-i(\vec{k}-\vec{q}) \cdot \vec{r}} \\ &= \frac{-1}{n_a^2 (2\pi)^{2m}} \int d^m r \int d^m q n_\nu(\vec{q}) \int d^m k [\vec{\partial}_k \cdot \vec{\partial}_k n_\nu(\vec{k})] (-\vec{\partial}_k \cdot \vec{\partial}_k)^{n-1} e^{-i(\vec{k}-\vec{q}) \cdot \vec{r}} \\ &\vdots \\ &= \frac{(-1)^n}{n_a^2 (2\pi)^{2m}} \int d^m k \int d^m q n_\nu(\vec{q}) [(\vec{\partial}_k \cdot \vec{\partial}_k)^n n_\nu(\vec{k})] \int d^m r e^{-i(\vec{k}-\vec{q}) \cdot \vec{r}} \\ &= \frac{(-1)^n}{n_a^2 (2\pi)^m} \int d^m k n_\nu(\vec{k}) [(\vec{\partial}_k \cdot \vec{\partial}_k)^n n_\nu(\vec{k})]. \end{aligned} \quad (16)$$

In the stationary state the momentum distribution is given by Eq. (5) of the main text, i.e.

$$n_{\vec{k}} = \frac{\kappa_\sigma \Gamma}{4} \frac{n_\sigma}{(\delta/2)^2 + \Delta_{\vec{k}}^2} \quad (17)$$

with $\delta^2 = \kappa_\sigma \Gamma [\Gamma/\kappa_\sigma - (2n_\sigma - 1)]$ and $\kappa_\sigma = 4g^2/\gamma_a$. Hence as long as $\delta^2 > 0$, that is, as long as,

$$\frac{\gamma_a \Gamma}{4g^2} - (2n_\sigma - 1) \neq 0, \quad (18)$$

we find that \mathcal{X}_ν^n is a finite number for any n and ν implying that the correlations $\mathcal{C}(\vec{r}) = \langle a_0^\dagger a_{0+\vec{r}} \rangle$ decay faster than r^{-n} for any positive integer n as $r \rightarrow \infty$.

The only possibility that the correlation length could diverge is thus a case where $(2n_\sigma - 1) = \Gamma/\kappa_\sigma$, for which $n_{\vec{k}} \propto \Delta_{\vec{k}}^{-2}$. For this case, however, the last term in Eq. (4b) in the main text, which reads $(2n_\sigma - 1) \frac{1}{n_a (2\pi)^m} \int_{V_k} d^m k F_{\vec{k}} n_{\vec{k}}$, diverges as long as $(2n_\sigma - 1) \neq 0$. The origin of this divergence is that $\Delta_{\vec{k}}^{-2}$ at least scales as $\Delta_{\vec{k}}^{-2} \propto (k_\alpha - \bar{k}_\alpha)^{-2}$ in the vicinity of a point \bar{k} where $\Delta_{\vec{k}} = 0$ (If $\Delta_{\vec{k}} = 0$ occurs at the boundary of the integration volume the divergence is even more severe). We thus conclude that non-exponential decay or a divergent correlation length can only appear for $\delta = 0$ and $(2n_\sigma - 1) = 0$. Both conditions can only hold for $\gamma_a = 0$, i.e. if the photon decay vanishes.

Estimates for field correlations in one dimension in the limit $N \rightarrow \infty$

For one dimension, $m = 1$, the momentum distribution in the stationary state reads, $n_k = \frac{\kappa_\sigma \Gamma}{4} \frac{n_\sigma}{(\delta/2)^2 + \Delta_k^2}$, which is a Lorentzian in the detunings $\Delta_k = \Delta - 2J \cos k$, and for $N \rightarrow \infty$ the field correlations read,

$$\mathcal{C}(x) = \frac{1}{n_a 2\pi} \int_{-\pi}^{\pi} dk e^{-ixk} n_k = \frac{1}{n_a \pi} \int_0^{\pi} dk \cos(xk) n_k, \quad (19)$$

where we have used $n_{-k} = n_k$ in the second equality. We now consider two cases, $|\Delta| < 2J$ and $|\Delta| = 2J$.

For $|\Delta| < 2J$ and large J , the momentum distribution is strongly peaked at $\Delta_k = 0$, that is at $k = \bar{k} = \cos^{-1}(\Delta/2J)$. We thus approximate Δ_k in the vicinity of $\Delta_k = 0$ by an expansion to linear order in $k - \bar{k}$ yielding $\Delta_k^2 \approx (4J^2 - \Delta^2) (k - \bar{k})^2$. Hence the momentum distribution n_k can be approximated by a Lorentzian distribution in $(k - \bar{k})$,

$$n_k \approx \frac{\kappa_\sigma \Gamma}{4(4J^2 - \Delta^2)} \frac{n_\sigma}{\lambda_1^2 + (k - \bar{k})^2}, \quad (20)$$

with $\lambda_1^2 = \frac{\delta^2}{4(4J^2 - \Delta^2)}$. For the field correlations we thus find,

$$\begin{aligned} \mathcal{C}(x) &= \frac{1}{n_a \pi} \Re \int_0^{\pi} dk e^{ixk} n_k \\ &\approx \frac{1}{n_a \pi} \Re \frac{\kappa_\sigma \Gamma n_\sigma e^{ix\bar{k}}}{4(4J^2 - \Delta^2)} \int_{-\infty}^{\infty} \frac{e^{ixp} dk}{\lambda_1^2 + (k - \bar{k})^2} \\ &= \frac{\kappa_\sigma \Gamma n_\sigma \cos(x\bar{k})}{4n_a \lambda_1 (4J^2 - \Delta^2)} e^{-\lambda_1 |x|}. \end{aligned} \quad (21)$$

Here we have extended the integration limits to infinity since the n_k rapidly approach zero as $|k - \bar{k}|$ grows. Hence

the correlations decay exponentially with the decay coefficient

$$\lambda_1 = \sqrt{\frac{g^2 \Gamma}{\gamma_a (4J^2 - \Delta^2)} \left[\frac{\gamma_a \Gamma}{4g^2} - (2n_\sigma - 1) \right]}, \quad (22)$$

and a periodic modulation $\cos(x\bar{k})$. Note that since $|\Delta| < 2J$ and $n_k \geq 0$ for all k , we always have $\lambda_1 > 0$. Also, note that for $\Delta^2 \propto J^2$ we have $\lambda_1 \propto J^{-1}$.

For $\Delta = 2J$ and large J , the distribution n_k is strongly peaked at $k = 0$ and we can approximate Δ_k in the vicinity of this peak by an expansion to leading order in k yielding $\Delta_k^2 \approx J^2 k^4$ and for the momentum distribution,

$$n_k \approx \frac{\kappa_\sigma \Gamma}{4J^2} \frac{n_\sigma}{\beta^2 + k^4}, \quad (23)$$

now with $\beta^2 = \frac{\delta^2}{4J^2}$. For the field correlations we thus find,

$$\begin{aligned} \mathcal{C}(x) &= \frac{\kappa_\sigma \Gamma n_\sigma}{4n_a J^2 (2\beta)^{3/2}} \left[\cos \left(\sqrt{\frac{\beta}{2}} |x| \right) + \sin \left(\sqrt{\frac{\beta}{2}} |x| \right) \right] \\ &\times e^{-\sqrt{\frac{\beta}{2}} |x|} \end{aligned} \quad (24)$$

Hence correlations decay exponentially with decay coefficient

$$\lambda_2 = \left\{ \frac{g^2 \Gamma}{4\gamma_a J^2} \left[\frac{\gamma_a \Gamma}{4g^2} - (2n_\sigma - 1) \right] \right\}^{\frac{1}{4}}. \quad (25)$$

Note that $\lambda_2 \propto J^{-1/2}$.

Examples for the fits

In this section we provide some examples for the fits of functions $f(x) = [c_1 \cos(\nu x) + c_2 \sin(\nu x)] \exp(-\lambda x)$ to the normalized correlations $\mathcal{C}(x)$. These examples are shown in Fig. 1 and illustrate the excellent quality of the fits. Only for $J \ll g$ the fitting procedure is more fragile as correlations decay very fast and are thus indistinguishable from zero for most values of x .

III. Derivation of the emitter spectrum of emission

In this section we obtain the emitter photoluminescence spectrum $S(\Gamma_d, \omega)$, in the lasing regime, where Γ_d is the detector linewidth. We make the semiclassical approximation of substituting the cavity fields by a multimode laser that acts independently on each of the emitters. That is, we consider the approximated Hamiltonian $H_{\text{ML}} = \sum_{\vec{r}} [\omega_\sigma \sigma_{\vec{r}}^\dagger \sigma_{\vec{r}} + \Omega(t) \sigma_{\vec{r}}^\dagger + \Omega^*(t) \sigma_{\vec{r}}]$, where $\Omega(t) = \sum_{\vec{k}} g \sqrt{n_{\vec{k}}/N} e^{-i\omega_{\vec{k}} t}$ is the time-dependent multimode field. Additionally, the emitters are still being excited by the incoherent pump and decay that act on their

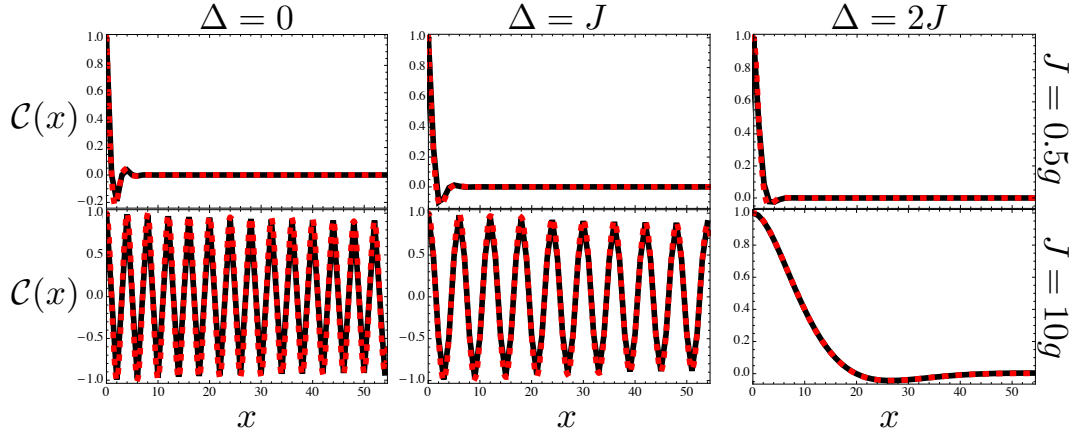


FIG. 1. Examples for fits of functions $f(x) = [c_1 \cos(\nu x) + c_2 \sin(\nu x)] \exp(-\lambda x)$ to the normalized correlations $\mathcal{C}(x)$ for $N = 108$ and the parameters Δ and J given in the labels of the columns and rows. Other parameters are $\gamma_a = 0.1g$, $\gamma_\sigma = 0.01g$, $P_\sigma = 5g$.

dynamics through the usual Lindblad forms. There is no steady state for this approximated model (for $N > 1$) but a quasi-steady state, that is, an ever oscillating solution for the density matrix elements around a mean point. Such mean point is given (approximately) by the exact solution of the full master equation or the rate equations, which do have a steady state. That is, $\sum_{\vec{k}} G_{\vec{k}\vec{r}} \langle p_{\vec{k}} \sigma_{\vec{r}}^\dagger \rangle e^{-i\omega_{\vec{k}} t}$ is well estimated by $\Omega(t) \langle \sigma_{\vec{r}}^\dagger \rangle_{ML}$, where $\langle \cdot \rangle_{ML}$ is the mean value obtained with the approximated master equation and Hamiltonian H_{ML} for the emitters only. The fact that the first term is \vec{r} -independent, compels $\Omega(t)$ to be \vec{r} -independent as well. We describe the resulting time-dependent dynamics in the following way: First, we solve the new master equation

with H_{ML} , and obtain its time-dependent spectrum of emission [48, 49], $S_{ML}(\Gamma_d, \omega, t)$, by coupling the emitter very weakly to another two-level system, which radiatively decays at a rate Γ_d , and plays the role of the detector. The population of this detector is exactly the time-dependent spectrum of our emitter [50]. Then, we take its average over time, once the quasi-steady state is reached, starting at a point in time which we call t_0 : $S(\Gamma_d, \omega) \approx \int_{t_0}^{t_0+T} S_{ML}(\Gamma_d, \omega, t) dt / T$. This is a very good approximation in the case $N = 1$ [17, 29] for which there is a simple analytical formula [45]. The Rayleigh peak, produced by the elastically scattered cavity laser field, is pinned at the cavity frequency, $\omega = \omega_a$, and has a small linewidth given by the detector only Γ_d (as in this approximation the cavity has an infinitely long lifetime).